Human Exposure to Wireless Charging Systems for Electric Vehicles in Multistorey Carpark

Zixuan Feng, Yinliang Diao
College of Electronic Engineering
South China Agricultural University
Guangzhou, China
diaoyinliang@ieee.org

Weinong Sun, Yaqing He, Peter Sai Wing Leung
Department of Electronic Engineering
City University of Hong Kong
Hong Kong SAR
eeswl@cityu.edu.hk

***Abstract*—This paper presents a study on the *in-situ* electric field strength inside the human body due to the exposure to low-frequency magnetic field generated by the wireless charging system (WCS) for electric vehicle inside a multistorey carpark. As the permeability of concrete is the same as that of air, the magnetic field generated by the WCS will penetrate through the floor under the primary coil, and hence result in an intense magnetic field downstairs. In this paper, the magnetic field strength, as well as the induced electric field strength inside a human body standing downstairs, are numerically assessed; the effect of the steel rebars on the dosimetry quantities is also investigated.**

Keywords—wireless charging; electric vehicle; low frequency; magnetic exposure; SPFD

I. Introduction

The wireless charging systems (WCS) for Electric Vehicles (EVs) utilizing induction coupling is developing rapidly [1], which has been adopted as an alternative to direct charging through cables. The maximum transmitting power for charging EVs could be as large as tens of kilowatts, and the operating frequency is typically in the range of kHz to several MHz.

Due to the intense magnetic field generated by the large charging current on the coils, there is a growing concern about the electromagnetic field (EMF) safety issues. The International Commission on Non-Ionizing Radiation Protection (ICNIRP) specifies the exposure limits basically in terms of reference level (RLs) and basic restrictions (BRs) [2]. Several studies have revealed that the exceedance of RLs for WCS of EV around the charging vehicle [3], [4]. Therefore, the assessment of induced *in-situ* electric field inside a human body is a necessity, in accordance with the guidelines.

Studies on exposure assessment have been carried out widely [3]–[7], these studies mainly focus on the safety of a human standing near the WCS. The WCS is generally installed on the floor underneath a vehicle, since the relative permeability of the concrete is about 1, the magnetic field generated by the WCS will penetrate through the floor under the primary coils, and hence result in an intense low-frequency (LF) magnetic field in the storey below. The time-varying LF magnetic field induces electric field inside human body standing below. Therefore, there is concern whether there is overexposure taking place in the space below the WCS.

In this study, we numerically calculated the induced electric field inside a human body standing downstairs and directly under a WCS. The effect of the steel rebars inside the floor slab was also investigated.

II. Models and Methods

A. WCS and Vehicle Models

In this study, the operation frequency of the WCS is set to be 80 kHz, in accordance with previous studies [7]. Reference [8] shows that the measured charging current on a 10-turn primary coil is 100 A, corresponding to a 6.6 kW charging system; these parameters are adopted in this study. The geometrical details of the WCS are shown in Fig. 1. A steel shield is placed between the secondary coil and the car model. The model of the electric vehicle is also shown in Fig. 1. The material of the car is set to be steel. Previous studies have revealed that a misalignment between the primary and the secondary coil leads to higher leakage of magnetic field, a misalignment of 20 cm is hence adopted here.

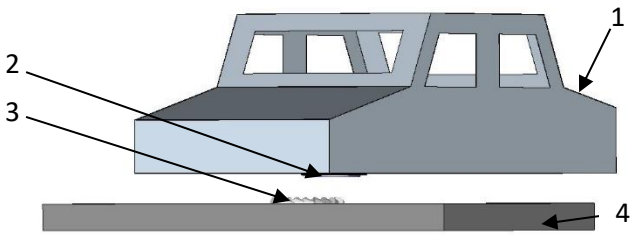

Fig. 1. WCS and vehicle models, 1. car model; 2. secondary coil and steel shield; 3. primary coil; 4. floor slab.

B. The floor slab model

Two different floor slab models, with and without the steel rebars, are adopted in this study to evaluate the effect of the floor slab on the magnetic field in the below space. The load-bearing reinforcement structure in the floor slab is composed of three parts: straight bars, negative reinforcements, and truss bars. The geometrical details of the rebars are provided in Fig. 2. The thickness of the floor slab is set to be 20 cm. The magnetic permeabilities of different materials adopted in this study are summarized in Table I.

TABLE I. RELATIVE PERMEABILITY OF MATERIALS

Material	Relative Permeability μ_r
Concrete	1.0
Air	1.0
Copper	1.0
Steel	1000.0

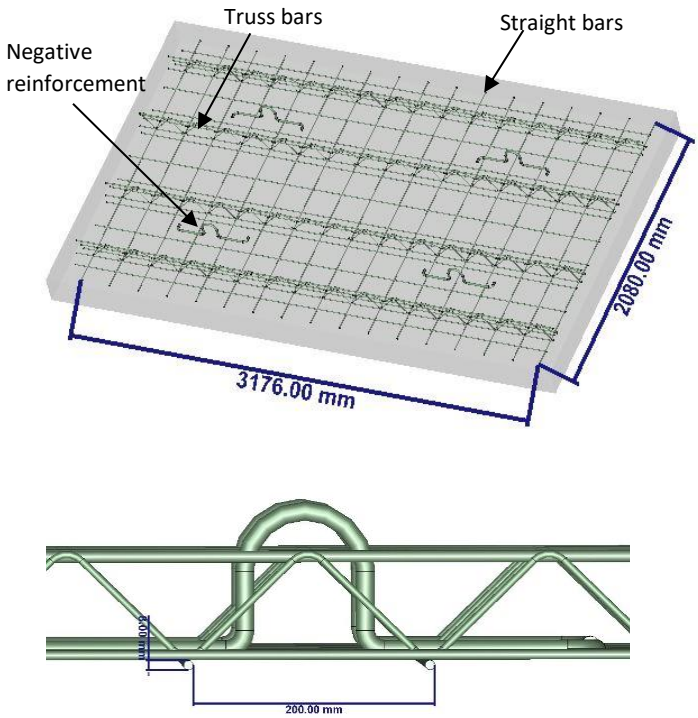

Fig. 2. Geometrical details of steel rebars in floor slab.

C. Human body model

The Japanese male model [9] is used in this study, with tissue dielectric properties adopted from [10]. The original spatial resolution of the male model is 2 mm; it is resampled at a resolution of 4 mm to speed up the convergence of numerical calculations in this paper. The human body model is placed at different distances below the floor slab, six cases, 0.4, 8, 15.2, 22.4, 29.6, and 36.8 cm are considered - the closest distance between the head and floor slab is 0.4 cm, the farthest distance is 36.8 cm.

D. In-Situ Electric Field Calculation

The magnetic field generated by the WCS without the human models is first simulated - three Cartesian components of the magnetic flux density *B* are calculated with a grid size of 4 mm, which is the same as the resampled human model. The vector potentials *A* are then calculated by (1) and then used as an equivalent source in the subsequent scalar potential finite difference (SPFD) calculations for induced electric field in the human model.

$$\begin{aligned} A_x &= \int_0^z B_y(x,y,t)dt \\ A_y &= \int_0^x B_z(s,y,0)ds - \int_0^z B_x(x,y,t)dt \\ A_z &= 0 \end{aligned} \tag{1}$$

The unknowns in SPFD are the scalar potentials ϕ at the nodes of each voxel, and they are solved by (2) iteratively using the Jacobi iterative method.

$$(\sum_{r=1}^{6}\bar{\sigma}_r)\phi_0 - \sum_{r=1}^{6}\bar{\sigma}_r\phi_r = j\omega d\sum_{r=1}^{6}(-1)^{r+1}\bar{\sigma}_r A_{0r} \tag{2}$$

where ϕ_r is the unknown scalar potential, $\bar{\sigma}_r$ is averaged conductivities of four voxels contacting edge *r*, *d* is the voxel side length and A_{0n} denotes the component of magnetic vector potential tangential to *the* edge. The electric field along the side of the voxel is then obtained by using (3).

$$\mathbf{E} = -j\omega\mathbf{A} - \nabla\phi \tag{3}$$

The electric field is then averaged over each voxel. The 99th percentile values of the induced electric fields are also evaluated.

III. RESULTS

A. Magnetic Flux Density

The magnetic flux density distributions are shown in Fig. 3(a) and Fig. 3(b) for the floor slab with and without rebars respectively. In Fig. 3, the black curves indicate the exposure at RLs for general public specified by ICNIRP-2010, and the yellow curves indicate the RLs of ICNIRP-1998. As can be observed, in the case of the floor slab without rebars, the ICNIRP RLs are exceeded in a large area below the charging WCS, while for the case with rebars, the area of overexposure is much smaller than the case without rebars. The steel rebars notably diminish the magnetic field that penetrates through the floor slab. For both cases, overexposure can happen in the storey below the WCS; this suggests that extra measurements and protections should be considered when installing WCS in a multistorey carpark. The maximum exposure is seen clearly to be the case when the human model is positioned closest to the floor slab.

B. In-Situ Electric Field

The induced electric field distribution inside the Japanese male model positioned at different distances below the floor slab is shown in Fig. 4. It can be seen that the LF magnetic field induces the highest electric field in the head of the human model since the head is the nearest part to the WCS. The 99th percentile electric field values are also calculated for comparison with the guidelines. The 99th percentile values of electric field and current density are reported in Table II.

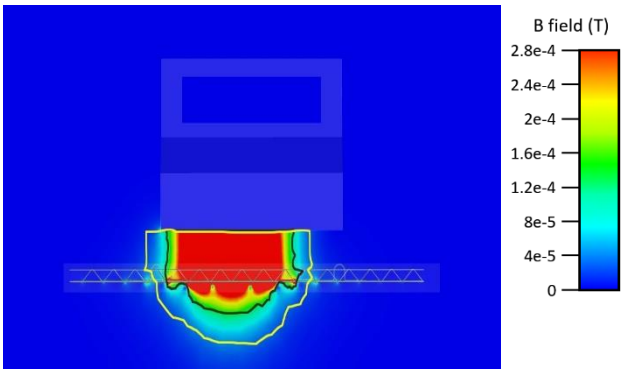

(a)

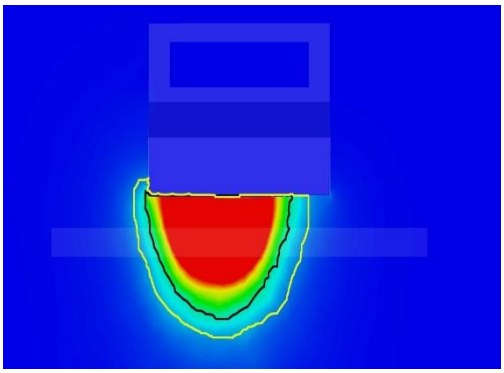

(b)

Fig. 3. Magnetic flux density distributions around a charging WCS: (a) floor slab with steel rebars, (b) floor slab without rebars.

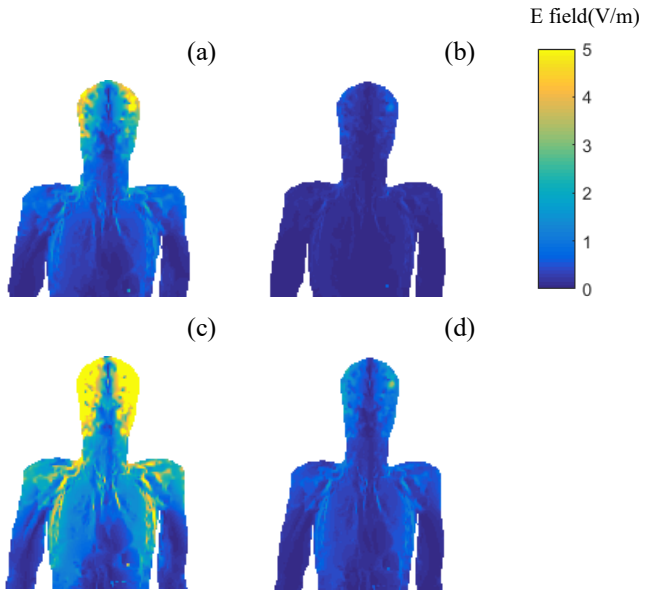

Fig. 4. Induced electric field distributions in the human body under the WCS: (a) 0.4 cm separation, with rebars, (b) 36.8 cm separation, with rebars, (c) 0.4 cm separation, without rebars, (d) 36.8 cm separation, without rebars.

TABLE II. 99TH PERCENTILE VALUES OF ELECTRIC FIELD AND CURRENT DENSITY IN HUMAN BODY

Separation (cm)	99th Percentile Values of Electric Field (V/m)		99th Percentile Values of Current Density (A/m^2)	
	With rebars	*Without rebars*	*With rebars*	*Without rebars*
0.4	4.8	12.2	0.68	1.8
8	2.9	7.8	0.42	1.2
15.2	1.9	5.4	0.28	0.84
22.4	1.3	3.8	0.19	0.61
29.6	0.86	2.7	0.14	0.46
36.8	0.60	2.0	0.098	0.35

As can be seen, for the case of the floor slab with steel rebars, the 99th percentile values of electric field are well within the BR limits for both occupational and general public exposures of ICNIRP-2010 (21.6 V/m for occupational exposure, 10.8 V/m for general public exposure). If the results are compared with ICNIRP-1998 BRs (0.8 A/m^2 for occupational exposure, 0.16 A/m^2 for general public exposure), the 99th percentile values of current density exceed BR for public exposure when the separation of human body and floor slab is less than ~25 cm for the case with rebars.

For the case of the floor slab without rebars, the 99th percentile value of electric field is 12.2 V/m when the human model is positioned closest to the floor slab. Exceedance of the ICNIRP-2010 BR for general public exposure only take place when the humans are placed closest to the source. The 99th percentile value of current density is 0.35 A/m^2 when the human model is positioned farthest from the floor slab, indicates that all the obtained 99th values exceed the BRs when compared with the ICNIRP-1998 BRs.

IV. CONCLUSION

In this paper, the external magnetic field and the induced electric field inside the Japanese male model stands below two different kinds of floor slabs with the wireless charging devices are investigated. The results first show that the steel rebars can notably reduce the magnetic field strength below the floor slab. Analysis of the obtained induced fields suggests that the ICNIRP-2010 BR can be exceeded when the human model is positioned close to the WCS above the head. The exceedance of ICNIRP-1998 BR can be observed when the separation of body and floor slab is larger than ~40 cm for the case without steel rebars, as ICNIRP-1998 is more conservative than ICNIRP-2010. The simulation results of this study clearly show that the LF magnetic field generated by the WCS can penetrate through the floor slab and leads to overexposure in the space below. Therefore extra measurements and shields should be considered when installing WCS in a multistorey carpark.

REFERENCES

[1] S. Li and C. C. Mi, “Wireless Power Transfer for Electric Vehicle Applications,” IEEE J. Emerg. Sel. Top. Power Electron., vol. 3, no. 1, pp. 4–17, Mar. 2015.

[2] ICNIRP-2010, “Guidelines for limiting exposure to time-varying electric and magnetic fields (1 Hz to 100 kHz).,” Health Phys., vol. 99, no. 6, pp. 818–36, Dec. 2010.

[3] T. Shimamoto, I. Laakso, and A. Hirata, “In-situ electric field in human body model in different postures for wireless power transfer system in an electrical vehicle.,” Phys. Med. Biol., vol. 60, pp. 163–173, 2015.

[4] I. Laakso, S. Tsuchida, A. Hirata, and Y. Kamimura, “Evaluation of SAR in a human body model due to wireless power transmission in the 10 MHz band,” Phys. Med. Biol., vol. 57, no. 15, p. 4991, 2012.

[5] A. Hirata, F. Ito, and I. Laakso, “Confirmation of quasi-static approximation in SAR evaluation for a wireless power transfer system.,” Phys. Med. Biol., vol. 58, pp. N241-9, 2013.

[6] A. Christ, M. Douglas, J. Nadakuduti, and N. Kuster, “Assessing human exposure to electromagnetic fields from wireless power transmission systems,” Proc. IEEE, vol. 101, no. 6, pp. 1482–1493, 2013.

[7] T. Sunohara, A. Hirata, I. Laakso, and T. Onishi, “Analysis of in situ electric field and specific absorption rate in human models for wireless power transfer system with induction coupling,” Phys. Med. Biol., vol. 59, no. 14, p. 3721, 2014.

[8] O. C. Onar, S. L. Campbell, L. E. Seiber, C. P. White, and M. Chinthavali, “A High-Power Wireless Charging System Development and Integration for a Toyota RAV4 Electric Vehicle,” 2016.

[9] T. Nagaoka, S. Watanabe, K. Sakurai, E. Kunieda, M. Taki, and Y. Yamanaka, “Development of realistic high-resolution whole-body voxel models of Japanese adult males and females of average height and weight, and application of models to radio-frequency electromagnetic-field dosimetry,” Phys. Med. Biol., vol. 49, no. 1, p. 1, 2003.

[10] S. Gabriel, R. W. Lau, and C. Gabriel, “The dielectric properties of biological tissues: III. Parametric models for the dielectric spectrum of tissues,” Phys. Med. Biol., vol. 41, no. 11, p. 2271, 1996.

